A real-time energy management system for smart grid integrated photovoltaic generation with battery storage

Chee Lim Nge[*], Iromi U. Ranaweera, Ole-Morten Midtgård, Lars Norum

Department of Electric Power Engineering, Norwegian University of Science and Technology, 7491 Trondheim, Norway

ARTICLE INFO

ABSTRACT

This paper proposes a real-time energy management system (EMS) suitable for rooftop PV installations with battery storage. The EMS is connected to a smart grid where the price signals indirectly control the power output of the PV/battery system in response to the demand variation of the electricity networks. The objective of the EMS is to maximize the revenue over a given time period while meeting the battery stored energy constraint. The optimization problem is solved using the method of Lagrange multipliers. The uniqueness of the proposed EMS remains in the reactive real-time control mechanism that compensates for the PV power forecast error. The proposed EMS requires only forecasting the average PV power output over the total optimization period. This is in contrast to the predictive power scheduling techniques that require accurate instantaneous PV power forecast. The proposed EMS method is verified by benchmarking against the predictive brute-force dynamic programming (DP) approach. The simulation analysis considers days with varying solar irradiance profiles. The simulation analysis shows the proposed EMS operating under practical assumptions, where the battery storage capacity is subject to constraints and the PV power output is not known *a priori*.

© 2018 Elsevier Ltd. All rights reserved.

1. Introduction

Due to the intermittency of PV, large-scale deployment of distributed PV generation poses technical challenges to the grid. High penetration levels of distributed PV generation cause reverse power flow in the distribution networks. This leads to the problem of voltage rise, as demonstrated in simulation analyses using actual load and solar irradiance data [1], [2]. Reverse power flow also introduces additional loading and power losses in the distribution transformers and the primary feeder sections [3], [4]. Mitigating these challenges will reduce grid reinforcement costs and operational costs [5].

To operate as a dispatchable generator similar to the conventional power sources, PV systems need energy storage device to balance the intermittency. The energy storage unit is used to balance intermittent PV generation. It stores the excess PV power when solar irradiance is abundant or when load consumption is low. On the other hand, it discharges when the demand rises or when PV ceases generation.

The techniques for finding a solution to the power scheduling problem of PV with energy storage encompass the traditional mathematical approaches and the modern approaches of artificial intelligence. The method of Lagrange multipliers is a mathematical technique for optimization problems subject to constraints. The Lagrange relaxation method is used to solve the optimal dispatch and security-constrained unit commitment problems of a PV/battery in a large power system with thermal units in Ref. [6]. In Ref. [7], a linear programming routine is used to minimize the grid power flow in a PV/battery system in real-time when the residential load exceeds the PV production. Furthermore, Ref. [7] adds a simple scheduling strategy to charge the battery during off-peak pricing period and discharge the battery during on-peak pricing period. Linear programming is also used in Ref. [8] to schedule different energy sources (a PV, a conventional energy source and a battery storage) and optimize the profit. The power path and conversion losses are assumed negligible in Refs. [7,8], hence providing only linear functions in the constraints and objective functions. In order to account for the nonlinear input—output characteristics and the discrete working ranges of the building energy systems, mixed-integer nonlinear programming is utilized in Ref. [9] to optimize the scheduling of grid-connected energy

---

* Corresponding author.
E-mail addresses: chee.lim.nge@gmail.com (C.L. Nge), iromi.ranaweera@ntnu.no (I.U. Ranaweera), ole-morten.midtgard@ntnu.no (O.-M. Midtgård), norum@ntnu.no (L. Norum).

systems consisting of PV and thermal energy storage. Dynamic programming technique is used in Ref. [10] for PV/battery scheduling with the objective of minimizing the operational cost. The operational cost in Ref. [10] includes the battery replacement cost, and the monetary transaction for selling and buying the electricity. Quadratic programming algorithm is used in Ref. [11] to maximize the revenue of a residential PV/battery system. The PV/battery system is assumed connecting to a grid with pricing scheme that aims to minimize the reverse power flow and peak loading in Ref. [11].

The scheduling approaches presented in Refs. [8–11], are predictive algorithms where perfect forecast of PV generation is assumed available. In Ref. [12], the comparative analysis shows that the scheduling of PV with energy storage can be improved by reducing the PV forecasting error. The day-ahead scheduling problem for a system with PV/battery has been reformulated as a fuzzy optimization problem to account for PV generation uncertainty in Ref. [13]. A membership function that represents varying degrees of truth models the uncertain PV generation, which in turn yields a fuzzy objective function. The uncertainty in the renewable energy system scheduling problem can also be approached by utilizing robust approach [14] or chance-constrained programming [15]. A two-stage robust approach is used in Ref. [16] to schedule the building energy system with PV and thermal energy storage, in order to minimize the operational cost. The "budget of uncertainty" of the robust scheduling strategy that yields low average operation costs with small standard deviations needs *a priori* determination. In Ref. [17], a unit commitment problem of wind power generation is formulated as a chance-constrained two-stage stochastic program, where the risk level is determined *a priori*.

Distributed generation unit such as PV can be indirectly controlled via price signals in response to demand variation. This brings about market integration of PV generations, and the optimal power flow is achieved through market mechanism. The economics of price distortion due to the lack of exposure of retail customers to the spot prices is explained in Ref. [18]. Among the price-based demand response mechanisms are time-of-use pricing, critical-peak pricing and real-time pricing schemes [19], [20]. A market-based demand response model involves the end consumers in the bidding processes. Due to the complexity that arises from the large number of residential appliances that participate in demand response, the end consumers need an interface with the market structure consisting of aggregators as considered in Ref. [21] or a microgrid coordinator as proposed in Ref. [22].

This paper proposes an energy management system (EMS) for grid-connected PV inverters with battery storage. The EMS is connected to a smart grid that employs demand response model. The EMS has the objective of maximizing the total revenue over a given time period. This paper aims to address the limitation of predictive power scheduling approach that requires *a priori* knowledge of instantaneous PV power. The proposed EMS utilizes reactive real-time control mechanism to compensate for the PV power forecast error. For a 24-hour period power scheduling, the proposed EMS requires only the average daily PV power output.

The paper is organized as follows. Section 2 develops the system level power flow model for use in formulating the economic optimization problem of a PV/battery system. Dynamic programming (DP) method that is used as a benchmark for the proposed EMS is presented in Section 3. The DP method is a predictive brute-force approach that requires accurate instantaneous PV power to be known *a priori*. Section 4 presents the proposed EMS that uses the method of Lagrange multipliers for solving the constrained optimization problem. In order to enable the reactive real-time control mechanism, the proposed EMS uses linear approximation for the dispatch function and a direct method for the Lagrange multiplier

estimation. Section 5 provides a simulation analysis that compares the proposed EMS to the brute-force DP approach. Final discussion and conclusions are offered in Section 6.

2. System modeling

The battery-link topology as depicted in Fig. 1 is a variant of dc-link topology similar to that proposed in Ref. [23]. The battery module is connected directly at the dc-link between the two step-up converters. The first step-up converter boosts the PV voltage V_{pv} to the battery voltage V_b. The second step-up converter further boosts V_b to the dc-link voltage, V_{dcl}.

Fig. 2 depicts the basic circuit implementation of the conventional dc-link topology. The operating principles of the boost converter, the bidirectional dc-dc converter and the full-bridge PWM inverter are available in the power electronics textbooks, such as [24].

The system power flow of the battery-link topology is described in (1). The arrows besides the power variables P_{pv}, P_b, P_{ac}, P_g and P_d indicates the direction of positive power flow, where the variables are defined as follows. The terms P_{pv} and L_{pv} denote the power and the loss functions of the PV power path. The output of P_{pv} branches into the battery power path P_b and the ac power path P_{ac}. The variable L_{ac} is loss function of the ac power path. The variable L_b is loss function of the battery power path.

$$P_{pv} - L_{pv} = P_{ac} + L_{ac} + P_b + L_b \qquad (1)$$

where

$$P_p = P_{pv} - L_{pv} \qquad (2)$$

$$P_{ac} = P_g + P_d \qquad (3)$$

The ac power path P_{ac} is the sum of the grid power P_g and the local demand power P_d.

This section aims to establish the mathematical models for the power loss functions, and represent the system power flow as a simple mathematical function. This allows mathematically deriving the power flowing through each power path in the PV/battery system. The power flowing through each power path needs to be derived to solve the power scheduling problem.

Fig. 3 provides the experimental result of L_{ac} of a battery-link topology PV/battery inverter. The ac power path loss function L_{ac} of the battery-link topology is the aggregate of the boost converter and full-bridge inverter conversion losses. Each boost converter consists of a 680 μH inductor (labeled respectively as L_{B1} and L_{B2} in Fig. 2) and it operates at 50 kHz switching frequency. MOSFET IXTP42N25P is used as the switching device for both the boost converter and the full-bridge inverter. The flyback diode (labeled respectively as D_{B1} and D_{B2} in Fig. 2) in the boost converter is SDT06S60. The full-bridge inverter consists of two 1 mH inductors (labeled as L_I in Fig. 2).

This paper assumes the ac power path loss L_{ac} can be modelled as a quadratic curve-fit function, where the ac power output P_{ac} is the explanatory variable. The method of ordinary least squares can be used to estimate the unknown coefficients of the linear regression model [25]. The ac power path loss in a quadratic function can be written as

$$L_{ac} = \alpha P_{ac} + \beta P_{ac}^2 + \chi \qquad (4)$$

The quadratic function as given in (4) is used to model the experimental results where the estimated coefficients of the linear regression model are $\alpha = 3.69 \times 10^{-2}$, $\beta = 1.29 \times 10^{-3}$, $\chi = 5.23$.

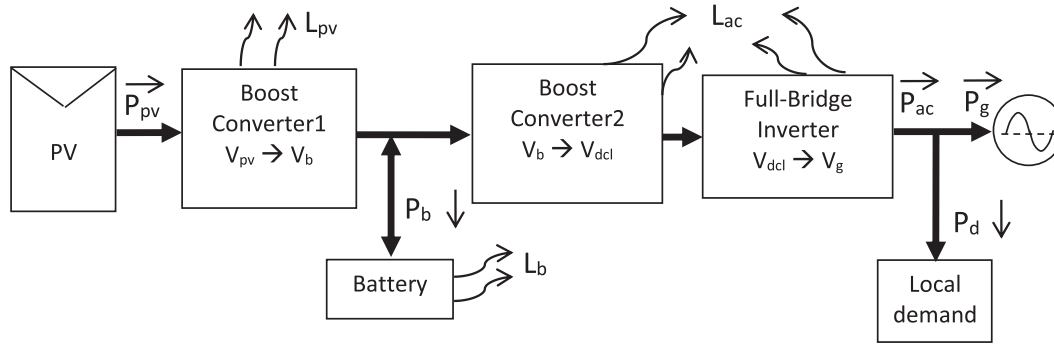This paper assumes lithium-ion battery, which has negligible
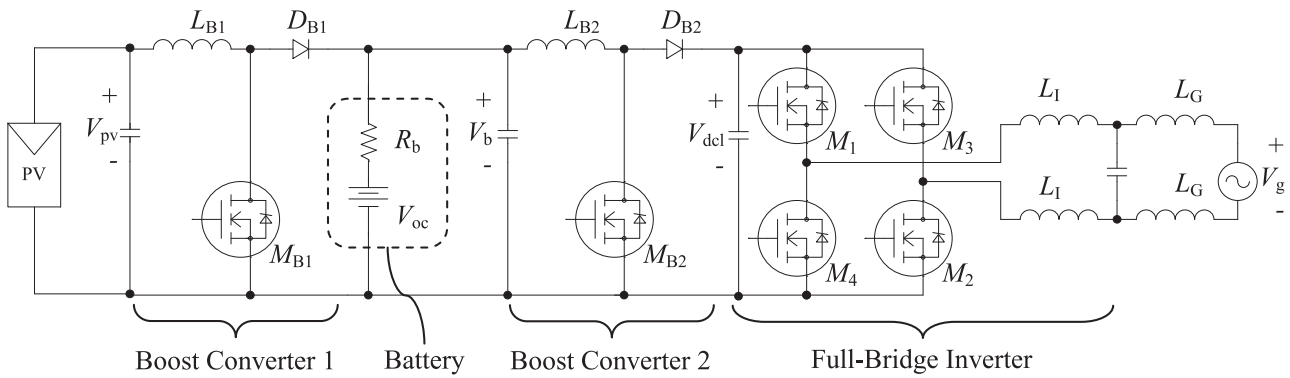
Fig. 1. Block diagram of battery-link topology.

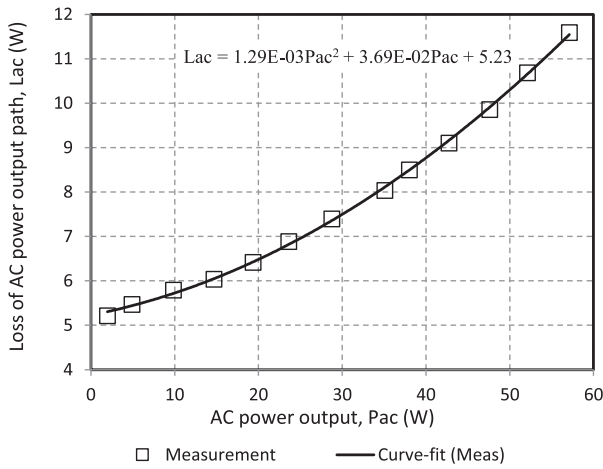**Fig. 2.** Circuit diagram of the conventional battery-link topology.

Fig. 3. Ac power path conversion losses in a battery-link topology.
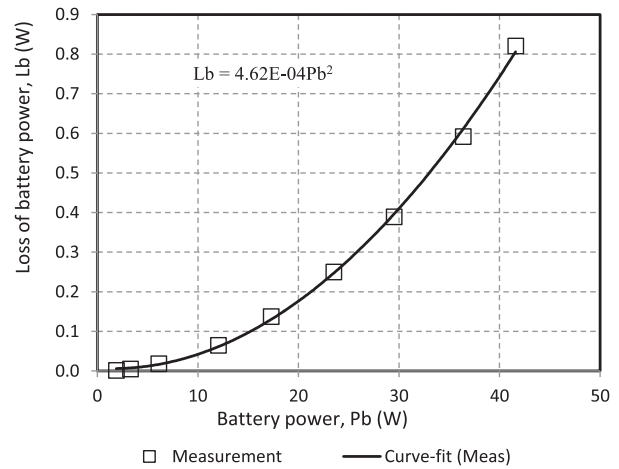

Fig. 4. Characteristic of battery power loss.

faradic power losses [26]. A lithium-ion battery module is used to obtain the experimental results of the battery loss L_b, as shown in Fig. 4. The lithium-ion battery module H2B182-B from HY-LINE AG is used to measure the battery power loss. Each battery module consists of four battery cells in series and three strings of cells in parallel. The lithium-ion battery cell is the popular 18650 cylindrical type, where the nominal voltage is 3.6 V. Two battery modules are connected in series to obtain 28.8 V nominal voltage. By observing the experimental results, we assume the battery loss L_b is proportional to the squared of the battery power

$$L_b = \kappa P_b^2 \tag{5}$$

where κ is a constant.

The loss function given in (5) is fitted to the empirical results where the coefficient κ of the curve-fit model equals 4.62×10^{-4}. By assuming that the models given in (4) and (5) provide sufficient curve-fitting accuracy, we can write the system power flow as a polynomial function

$$P_{p,t} = (\alpha + 1)P_{ac,t} + \beta P_{ac,t}^2 + \chi + P_{b,t} + \kappa P_{b,t}^2 \qquad (6)$$

3. Dynamic programming (DP)

This section presents the dynamic programming (DP) method that is used as a benchmark for the proposed EMS. The DP method presented here is based on the basic principles found in Refs. [27,28]. In order to apply the dynamic programming (DP) approach, the PV/battery scheduling problem is formulated as a multistage problem. The battery stored energy is the state variable. We wish to find the optimum trajectory of the battery stored energy states over a given time period that maximizes the total sum of revenues. Consider the battery stored energy states in two consecutive time intervals

$$E_{b,t,j} = P_{b,t}\Delta t + E_{b,t-1,i} \qquad (7)$$

for $i = 1, \ldots, N$ and $j = 1, \ldots, N$. The lower limit of the battery stored energy state is given as $E_{b,t,1}$ whereas the upper bound is given as $E_{b,t,N}$. Also, Δt is the step size of the time interval. The system operates in a liberalized electricity market where the electricity price $\pi_{g,t}$ is time variable. The revenue function for a given time interval is given as

$$R_t\left(E_{b,t,j}, E_{b,t-1,i}\right) = P_{g,t}\left(E_{b,t,j}, E_{b,t-1,i}\right)\pi_{g,t}\Delta t \qquad (8)$$

We consider the battery-link topology as shown in Fig. 1, in which the power loss model is provided in the previous section. The grid power $P_{g,t}$ as a function of the battery stored energy state can be obtained by substituting (3) and (7) in (6)

$$P_{g,t}\left(E_{b,t,j}, E_{b,t-1,i}\right) = \frac{\sqrt{(\alpha + 1)^2 + 4\beta c_{ij,t}} - \alpha - 1}{2\beta} - P_{d,t} \qquad (9)$$

where

$$c_{ij,t} = \kappa\left(\frac{E_{b,t,j} - E_{b,t-1,i}}{\Delta t}\right)^2 + \left(\frac{E_{b,t,j} - E_{b,t-1,i}}{\Delta t}\right) + \chi - P_{p,t}$$

Let $F_{t-1}(E_{b,t-1,i})$ be the maximum total sum of revenues up to the time interval $t-1$. Then, for arbitrary i and j battery stored energy states, the total sum of revenues at time interval t is

$$F_{t,ij} = R_t\left(E_{b,t,j}, E_{b,t-1,i}\right) + F_{t-1}\left(E_{b,t-1,i}\right) \qquad (10)$$

We wish to maximize the total sum of revenues over a given time period. An optimal choice of i is the one that maximizes $F_{t,ij}$ function. We thus obtain the basic recursive form functional equation for maximizing the total sum of revenues for a given time period as

$$F_t\left(E_{b,t,j}\right) = \max_{\{i\}}\left[R_t\left(E_{b,t,j}, E_{b,t-1,i}\right) + F_{t-1}\left(E_{b,t-1,i}\right)\right] \qquad (11)$$

The forward dynamic programming (DP) algorithm that maximizes the total sum of revenues over the given time period T is shown as a flow chart in Fig. 5. We introduce $S_t(E_{b,t,j})$ for storing the $t-1$ state $E_{b,t-1,i}$ that maximizes the total sum of revenues at t state $E_{b,t,j}$. A variable F_{max} is used to store the "maximum revenue so far" and track the optimal result in each i state iteration and it is reset to an arbitrary minimum value every time j is assigned a new value. Note that the DP algorithm is a predictive approach that requires accurate PV power to be known *a priori*. The instantaneous PV

output power $P_{p,t}$ is required to obtain the grid power $P_{g,t}$ as given in (9), which in turn is used to calculate the total revenue as given in (10).

4. Energy management system based on the method of Lagrange multipliers

The proposed EMS aims to provide a mean for reactive real-time control to the PV/battery system. Here we use the method of Lagrange multipliers to obtain a closed form expression for the optimal dispatch function. The objective function for maximizing the total sum of revenues over the given time period T can be written as

$$R_T = \max\sum_{t=1}^{T} R_t = \max\sum_{t=1}^{T} P_{g,t}\pi_{g,t}\Delta t \qquad (12)$$

The objective function is subject to the law of power conservation:

$$\phi_t = P_{p,t} - (\alpha + 1)P_{ac,t} - \beta P_{ac,t}^2 - \chi - P_{b,t} - \kappa P_{b,t}^2 = 0 \qquad (13)$$

The objective function is also subject to constraint that ensures the battery stored energy over the given time period meet the target $E_{b,T}$

$$\psi = \sum_{t=1}^{T} P_{b,t}\Delta t - E_{b,T} = 0 \qquad (14)$$

4.1. Method of Lagrange multipliers

The constrained optimization problem can be addressed using methods of calculus involving the Lagrange function $\mathscr{L}$ as follows:

$$\mathscr{L} = \sum_{t=1}^{T} P_{g,t}\pi_{g,t}\Delta t + \sum_{t=1}^{T} \lambda_t\phi_t + \gamma\psi \qquad (15)$$

where λ and γ are Lagrange multipliers.

For any given values of P_p and P_d the independent variables are P_g and P_b. The solutions for the partial derivatives of the Lagrange equation yield the optimum point

$$\frac{d\mathscr{L}}{dP_{g,t}} = \pi_{g,t}\Delta t - \lambda_t\left[2\beta(P_{g,t} + P_{d,t}) + (\alpha + 1)\right] = 0$$

$$\frac{d\mathscr{L}}{dP_{b,t}} = \gamma\Delta t - \lambda_t(2\kappa P_{b,t} + 1) = 0$$

$$\frac{d\mathscr{L}}{d\lambda_t} = \phi_t = 0 \qquad (16)$$

$$\frac{d\mathscr{L}}{d\gamma} = \psi = 0$$

We solve these two sets of constraints in two stages. The first stage is to find the solution for optimal dispatch problem and eliminate the first Lagrange multiplier λ. By solving the first three equations in (16), the solution for the battery power $P_{b,t}$ and the grid power $P_{g,t}$, at any given t are as follows:
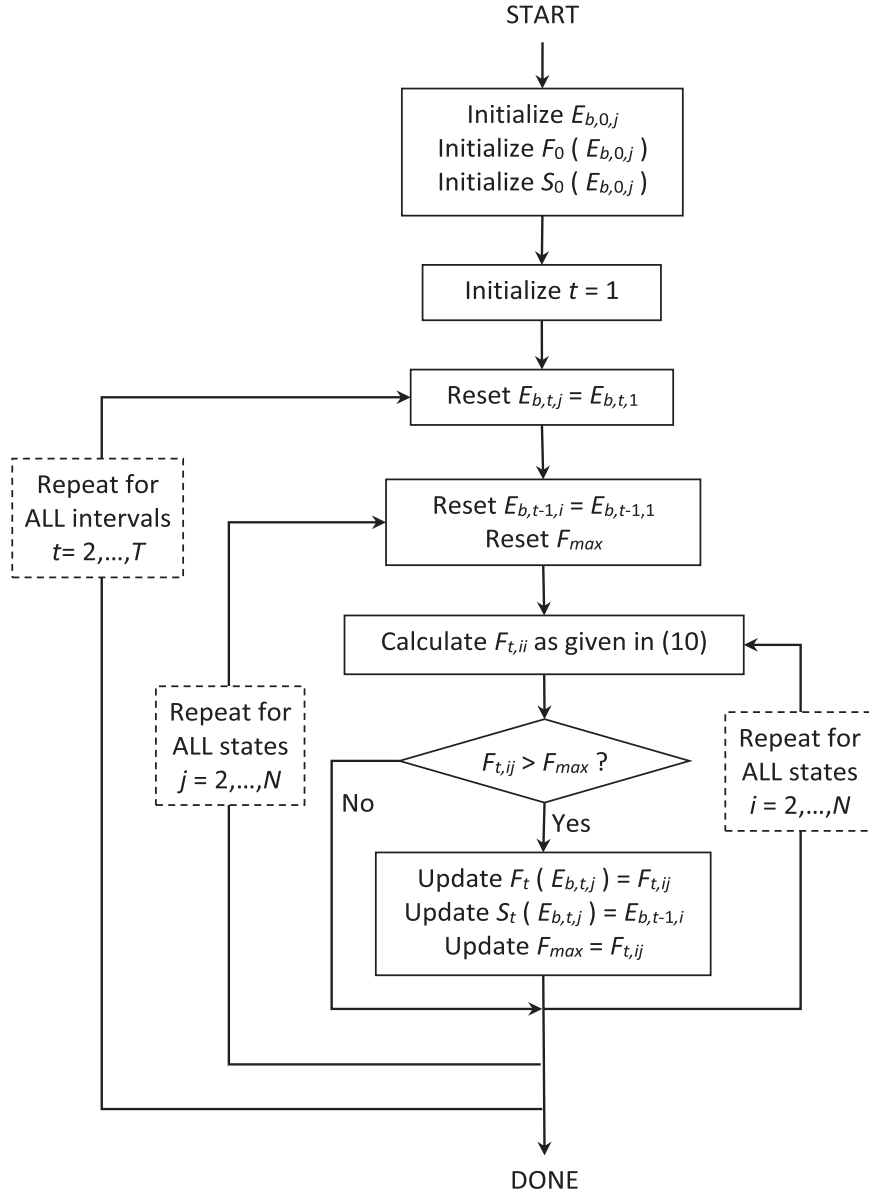
Fig. 5. Flow chart for solving the PV/battery scheduling problem using DP.

$$P_{b,t} = \frac{1}{2\kappa}\left[-1 + \sqrt{\frac{1 + 4\beta(P_{p,t} - \chi) + (\alpha+1)^2 - \left(\frac{\pi_{g,t}}{\gamma}\right)^2}{\left(\frac{\pi_{g,t}}{\gamma}\right)^2 + \frac{\beta}{\kappa}}} \right] \tag{17}$$

$$P_{g,t} = \frac{\pi_{g,t}\kappa}{\gamma\beta}P_{b,t} + \frac{1}{2\beta}\left(\frac{\pi_{g,t}}{\gamma} - \alpha - 1\right) - P_{d,t} \tag{18}$$

The second stage is to solve the daily scheduling by adjusting the Lagrange multiplier γ to satisfy the battery stored energy constraint $E_{b,T}$ as given in the last equation in (16). The dimension of the second Lagrange multiplier γ is analyzed by observing (18). The loss coefficients κ and β have no units, so we can conclude that γ has the same unit as the grid feed-in price π_g. We can infer that the Lagrange multiplier γ is the "shadow price" of the battery. The

Lagrange multiplier γ represents the total revenue the system would generate for increasing one unit of battery stored energy. Equation (18) gives a nonlinear relationship between the Lagrange multiplier γ and the battery power P_b. An iterative method is required to find the exact value of the Lagrange multiplier γ that satisfies the battery stored energy target $E_{b,T}$ as given in the last equation in (16). An iteration process using the gradient search method to solve for the Lagrange multiplier γ is presented in Ref. [29]. In order to enable the reactive real-time control mechanism in the proposed EMS, a direct method is developed to estimate the Lagrange multiplier γ as presented in the next subsection.

4.2. Proposed energy management system (EMS)

The results from the method of Lagrange multipliers are used to obtain the optimal dispatch function solution in closed form. The real-time battery power target value $P_{br,t}$ as a closed form optimal

dispatch function is the linear approximation of the battery power $P_{b,t}$, as given in (17), at zero

$$P_{br,t} = \frac{\beta}{\kappa\left(\frac{\pi_{g,t}}{\gamma}\right)^2 + \beta} P_{p,t} + \frac{(\alpha+1)^2 - \left(\frac{\pi_{g,t}}{\gamma}\right)^2 - 4\chi\beta}{4\left[\kappa\left(\frac{\pi_{g,t}}{\gamma}\right)^2 + \beta\right]} \qquad (19)$$

Equation (19) is a computationally efficient linear equation. The dynamic variables in (19) are the PV power output $P_{p,t}$ and the electricity price signal $\pi_{g,t}$, which typically changes hourly.

Next, we wish to develop a direct method to estimate the Lagrange multiplier γ. We assume the power scheduling algorithm has a daily cycle time, that is, the optimization duration T corresponds to a 24-hour period. Let $\pi_{g,d}$ be a constant value representing the electricity price signal for a given day. Substituting the daily representative value $\pi_{g,d}$ as a constant for the time varying $\pi_{g,t}$ in (19), we estimate the second Lagrange multiplier as

$$\gamma \approx \pi_{g,d}\sqrt{\frac{4\kappa P_{b,d} + 1}{(\alpha+1)^2 + 4\beta\left(P_{p,d} - P_{b,d} - \chi\right)}} \qquad (20)$$

where $P_{b,d}$ is the average daily battery power and $P_{p,d}$ is the average daily PV power output. The daily representative electricity price $\pi_{g,d}$ and the average daily PV power output $P_{p,d}$ need to be obtained in advance. As part of the reactive control mechanism to compensate for the $P_{p,d}$ forecasting error, the average daily battery power $P_{b,d}$ is dynamically adjusted by comparing the battery stored energy target $E_{b,T}$ to the actual energy value at interval t

$$P_{b,d} = f_c\left(\frac{E_{b,T} - E_{b,t}}{T - t + 1}\right) \qquad (21)$$

where f_c is a scale factor used to convert the time variables, t and T, to units compatible with the battery stored energy variables $E_{b,t}$ and $E_{b,T}$.

The control configuration of the proposed EMS for a PV/battery system is shown in Fig. 6. The first boost converter is controlled by the voltage mode controller C_{pv}. The maximum power point tracker (MPPT) adjusts the reference signal to the voltage mode controller C_{pv} to ensure the PV module operates close to the maximum power point. The MPPT unit also provides the PV power output $P_{p,t}$ in real time to the EMS. The battery management system (BMS) sets the reference signals to the battery charge controllers C_{ibat} and C_{vbat}. The voltage mode controller C_{vbat} ensures that the predetermined upper limit of battery termination voltage is never exceeded. The battery charging and discharging current is adjusted by the current mode controller C_{ibat}, where the reference signal $I_{ref,bat}$ is derived from the EMS battery power target value $P_{br,t}$. The grid feed-in controller for the full-bridge inverter consists of two loops. The outer loop feed-forward controller C_{ff} regulates the power transfer between the full-bridge inverter and the second boost converter. The phase locked loop PLL generates a reference sine wave that is in phase with V_g. The inner loop controller C_{iac} regulates the ac output current of the full-bridge inverter to ensure it is in phase with the grid voltage. The EMS under real-time pricing scheme [19,20], communicates $\pi_{g,t}$ directly with the utility system operator every hour. For market structure that involves bidding processes, the EMS may communicate $\pi_{g,t}$ with the aggregator that bids on behalf of the PV/battery system [21].

Fig. 7 shows the proposed EMS reactive real-time control algorithm in a flow chart. After initialization, the program loops at a constant Δt time step to read the real-time PV power $P_{p,t}$ from the MPPT and then write the calculated battery power target value $P_{br,t}$

to the BMS. Note that the proposed EMS does not require the instantaneous PV power output forecast. Only the average daily PV power output $P_{p,d}$ needs to be forecasted as part of the initialization process. A hardware timer is assumed to ensure the program loops at a constant Δt time step.

The EMS algorithm steps that involve data passing between the EMS and other subsystems (such as the BMS) are highlighted with circled capital letters Ⓐ, Ⓑ, Ⓒ and Ⓓ in Figs. 6 and 7. On the other hand, the algorithm steps that involve calculation using the equations as given in (19)−(21) are highlighted with circled small letters ⓧ, ⓨ and ⓩ in Fig. 7. The main algorithm steps of the proposed EMS are summarized as follow:

Step 1 As part of the initialization process, the EMS resets the following variables at the beginning of each daily cycle
  ○ The average daily PV power output $P_{p,d}$ is forecasted
  ○ The daily representative value for the electricity prices $\pi_{g,d}$ is estimated
  ○ The initial value for the time variable t is reset to 1
  ○ The initial value for the loop counter q is reset to the end value q_{last}

Step 2 The EMS reads the battery stored energy $E_{b,t}$ from the BMS. This process is indicated as Ⓐ in Figs. 6 and 7.

Step 3 The average battery power $P_{b,d}$ is adjusted by comparing the real time value $E_{b,t}$ (as read in Step 2) to the target value $E_{b,T}$. This step uses the equation as given in (21) and it is indicated as ⓧ in Fig. 7.

Step 4 The EMS reads the time varying $\pi_{g,t}$ from the utility system operator. This process is indicated as Ⓑ in Figs. 6 and 7.

Step 5 The Lagrange multiplier γ as the "shadow price" of the battery is calculated using the equation as given in (20). This step is indicated as ⓨ in Fig. 7. The variables are obtained in the previous steps:
  ○ The average daily PV power output $P_{p,d}$ iss forecasted in Step 1
  ○ The average daily battery power $P_{b,d}$ is calculated in Step 3
  ○ The time varying $\pi_{g,t}$ is read in Step 4

Step 6 The EMS reads the real-time PV power $P_{p,t}$ from the MPPT. This process is indicated as Ⓒ in Figs. 6 and 7.

Step 7 The battery reference set point power target value $P_{br,t}$ is calculated using the equation as given in (19). This step is indicated as ⓩ in Fig. 7. The variables are obtained in the previous steps:
  ○ The time varying $\pi_{g,t}$ is read in Step 4
  ○ The Lagrange multiplier γ is calculated in Step 5
  ○ The real-time PV power $P_{p,t}$ is read in Step 6

Step 8 The EMS writes the calculated battery power target value $P_{br,t}$ to the BMS. This process is indicated as Ⓓ in Figs. 6 and 7.

The Lagrange multiplier γ does not require rapid adjustment to compensate for the average daily PV power output $P_{p,d}$ forecasting error. The average daily battery power $P_{b,d}$ and the Lagrange multiplier γ are computed only when the loop counter q reaches the end value q_{last}. The EMS algorithm Steps 2−5, which are indicated as Ⓐ, Ⓑ, ⓧ and ⓨ in Fig. 7, are bypassed for each q increment iteration.

In summary, the proposed EMS continuously adjusts the battery power (by setting the power target value $P_{br,t}$) in order to achieve the objective of maximizing the total sum of revenues R_T and meeting the battery stored energy constraint target $E_{b,T}$ over a given time period. The EMS computes the battery power target value $P_{br,t}$ and sends it to the BMS for adjusting the battery charging and discharging current.
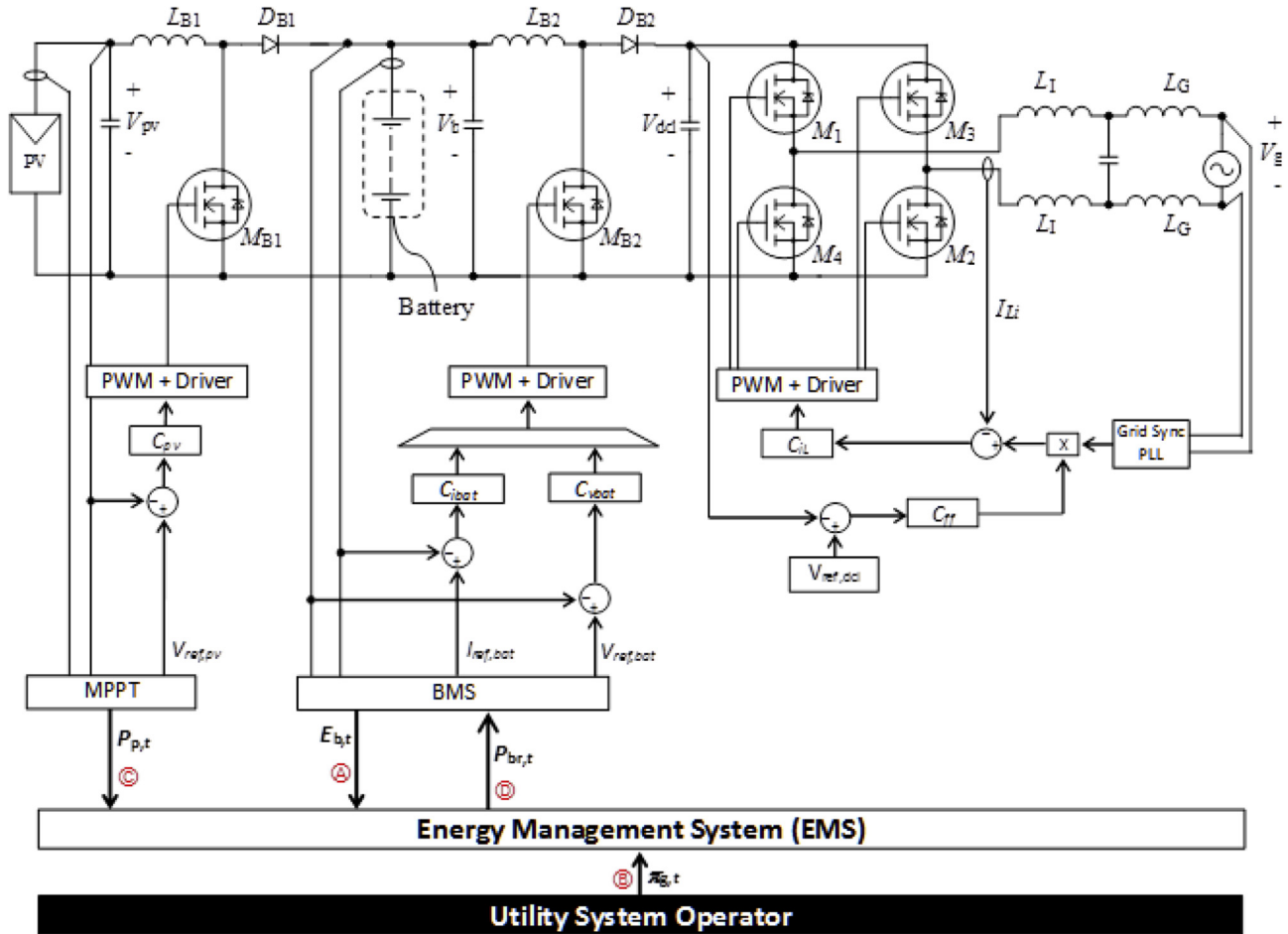
Fig. 6. EMS control configuration of battery-link topology.

5. Simulation analysis

This section presents the simulation analysis of PV/battery system power scheduling with the objective of benchmarking the proposed real-time EMS (as presented in Section 4) against the brute-force DP approach (as presented in Section 3). The DP and proposed EMS algorithms are simulated by implementing the flow charts (as shown in Figs. 5 and 7) in the Microsoft VBA (Visual Basic for Application) software. The power scheduling algorithms aim to maximize the total sum of revenues over a 24-hour period. The approach for assigning values to the parameters required for the calculation steps (as presented in Sections 3 and 4) are summarized here:

- The simulation time interval step size Δt is arbitrarily selected as 5 min.
- The time variable T is set equal to 288 since the algorithms aim to maximize the daily total revenue.
- The battery charge is cycled to the initial capacity for every 24-hour period to maximize the utilization of the battery. Hence, the target total battery stored energy constraint $E_{b,T}$ is set equal to zero.
- The coefficients of the mathematical models presented in Section 2 are derived from the experimental results. The coefficients for the ac power path loss L_{ac} quadratic function as given in (3) are $\alpha = 3.69 \times 10^{-2}$, $\beta = 1.29 \times 10^{-3}$, $\chi = 5.23$.

Additionally, the coefficient for the battery loss L_b given in (5) assumes the coefficient κ equals 4.62×10^{-4}.
- For the simulation of the DP approach, the battery stored energy state $E_{b,t}$ is incremented in a step size of 5/12 Wh. This provides 5 W granularity in the battery power $P_{b,t}$ calculation for 5 min of time interval step size Δt. Apparently, the increment size of $E_{b,t}$ determines the value of N, number states of the battery stored energy. For example, N shall be set to 6000 if $E_{b,t,1}$ equals 0 Wh, and $E_{b,t,N}$ equals 500 Wh.
- For the simulation of the proposed EMS, the loop counter end value q_{last} is set equal to 3 because 15 min of interval is arbitrarily selected for adjusting the Lagrange multiplier γ in order to compensate for the errors in the PV power forecast.
- For the simulation of the proposed EMS, the daily representative value for the electricity prices $\pi_{g,d}$ is set equal to the arithmetic mean of the hourly electricity prices.
- For the simulation of the proposed EMS, the average daily PV power output $P_{p,d}$ needs to be forecasted. One trivial forecast approach is the basic 24-hour persistence model [30,31], where $P_{p,d}$ of the current day is set (at the initialization stage) equal to the calculated value of $P_{p,d}$ of the previous day.

Fig. 8 shows the PV power output P_p obtained from the outdoor measurement results of a 1.71 m^2 poly-silicon PV module in Grimstad, Norway between July 10 and July 12, 2011. Days with varying solar irradiance profiles are chosen to illustrate the effect of forecast errors on the proposed EMS. The first two days (July 10 and
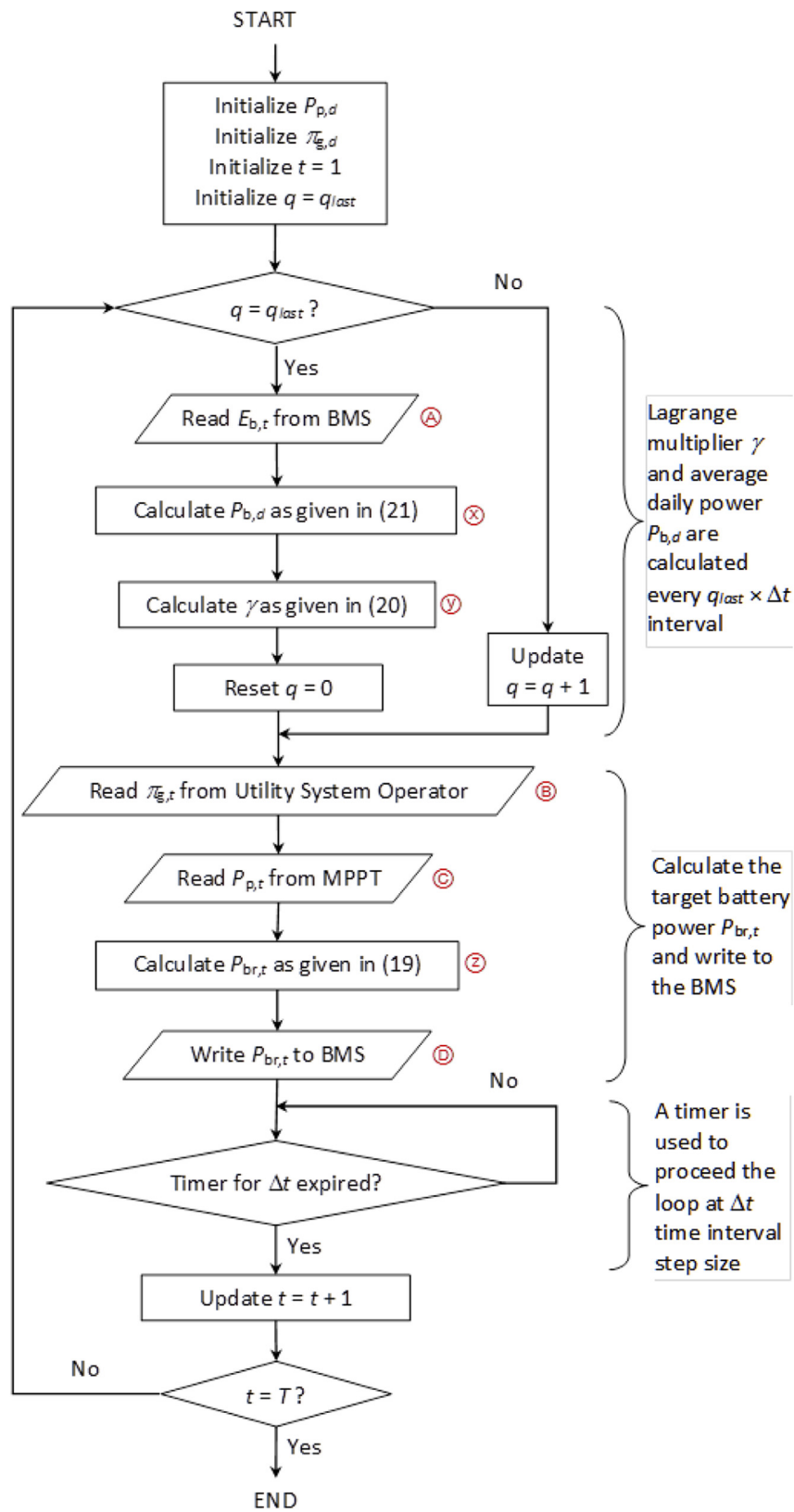
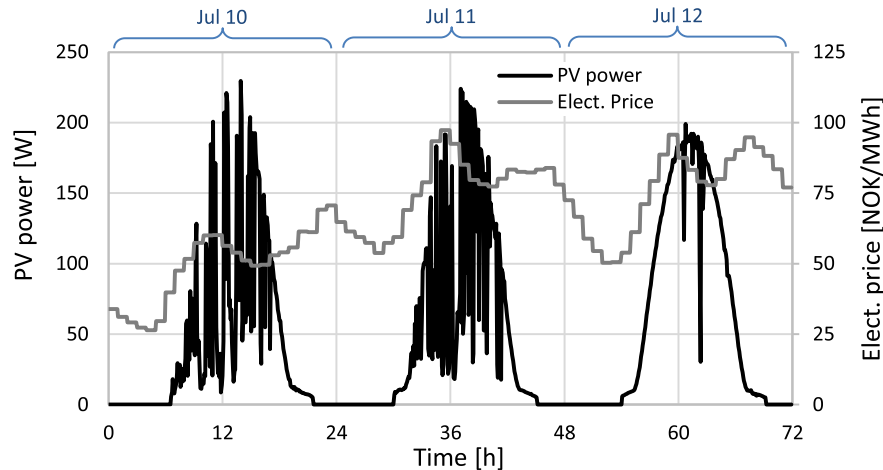**Fig. 7.** Flow chart of the proposed real-time EMS.

Fig. 8. Measured PV power $P_{p,t}$ and the electricity price $\pi_{g,t}$ for three consecutive days of July in Southern Norway.

July 11) have cloudy conditions whereas the third day (July 12) has a clear sky condition. The time-varying electricity price signal π_g for the simulation analysis is represented by the hourly electricity spot price of the Nord Pool day-ahead market [32] in the pricing area of Grimstad (Kristiansand), Norway between July 10 and July 12, 2015.

The comparative simulation analysis where the proposed real-time EMS operates under the ideal condition is first presented to validate the approximation methods. Fig. 9 shows the power scheduling simulation results assuming unconstrained battery energy capacity conditions. Also, the proposed EMS has *a priori* knowledge of the PV power for accurate forecasting of the daily average $P_{p,d}$ in the calculation of the Lagrange multiplier γ as given in (20). In order to provide a comparison for the daily total sum of revenues, the total revenue R_t is reset to zero Norwegian Krone (NOK) every day at the midnight. In Fig. 9, the power scheduling traces of the proposed EMS closely track those of the baseline DP. We can conclude that the approximations used in estimating the battery power target $P_{br,t}$ as given in (19), and the Lagrange multiplier γ as given in (20) yield negligible errors.

Next, we wish to show the proposed EMS operating under practical assumptions, where the battery storage capacity is subject to constraints and the PV power output is not known *a priori*. The average daily battery power $P_{b,d}$ and the Lagrange multiplier γ are adjusted every 15 min to compensate for the errors in the PV power forecast. For this simulation analysis, the basic 24-hour persistence forecast model [30,31], is used in the real-time EMS.

Fig. 10 shows the comparative simulation analysis considering the battery maximum capacity is limited to 500 Wh. July 10 and July 11 have similar daily average PV power output. Fig. 10a and b shows that the power traces ($P_{b,t}$ and $P_{ac,t}$) of the proposed EMS and the baseline DP track closely between t_0 and t_1. Since the battery stored energy $E_{b,t}$ is the integral of battery power $P_{b,t}$ over time, the errors in $E_{b,t}$ gradually increase. Between t_1 and t_2, the real-time EMS readjusts γ, and it increases $P_{b,t}$ in order to charge the battery to the initial 200 Wh battery capacity at t_2 (and meet the target $E_{b,T}$). On July 12, the proposed EMS charges the battery to the maximum limit of $E_{b,t}$ early on whereas the DP approach reaches the maximum capacity only at t_3. Since the proposed EMS uses the 24-hour persistence PV power forecast model, higher average PV power on July 12 is unforeseen by the proposed EMS. Even though $E_{b,t}$ continues to deviate after t_3, the proposed EMS manages to readjust γ toward the end of July 12 and meet the target $E_{b,T}$. Note also that the daily revenues R_t generated by the proposed EMS on July 11 and July 12 are similar to those generated by the baseline DP.

Given that a trivial PV power forecast model is implemented, the proposed EMS yields reasonable results in meeting the battery energy target $E_{b,T}$ while maximizing the revenues. We can conclude that the average daily battery power $P_{b,d}$ function as given in (21), which in turn adjusts the Lagrange multiplier γ, provides sufficient reactive real-time control for compensating the PV power forecasting errors.

The approximations used in the proposed EMS provide a computationally efficient real time control at the expense of less accurate optimization results. One the other hand, the DP method is a brute-force approach that assumes an accurate instantaneous PV power forecast is available. As shown in Figs. 9 and 10, the approximations used in the real-time EMS produce slight deviations of results between the proposed EMS and the brute-force DP approach. The approximations used in the proposed EMS are summarized as follow:

- The battery power target value $P_{br,t}$ as the dispatch function of the proposed EMS is a linear approximation.
- In order to use a direct method to approximate the Lagrange multiplier γ, the proposed EMS assumes the daily electricity price signal can be represented by a constant value $\pi_{g,d}$.
- The proposed EMS uses the arithmetic mean of the hourly electricity prices to approximate $\pi_{g,d}$.
- For simulation analysis under practical assumptions (where the results are as shown in Fig. 10), the proposed EMS estimates the average daily PV power output $P_{p,d}$ using the basic 24-hour persistence forecast model.

6. Conclusion

This paper presents a real-time energy management system (EMS), which maximizes the total revenue for the PV/battery system that connects to a smart grid with time varying electricity prices. The proposed EMS utilizes reactive real-time control mechanism to compensate for the PV power forecast error. Hence, it addresses the limitation of predictive PV power scheduling approach that requires an accurate instantaneous PV power forecast. The proposed reactive real-time control mechanism requires only forecasting the average PV power output over the total optimization period. The proposed EMS is based on the method of Lagrange multipliers, and the power scheduling algorithm is shown in Fig. 6. In order to enable the reactive real-time control, this paper
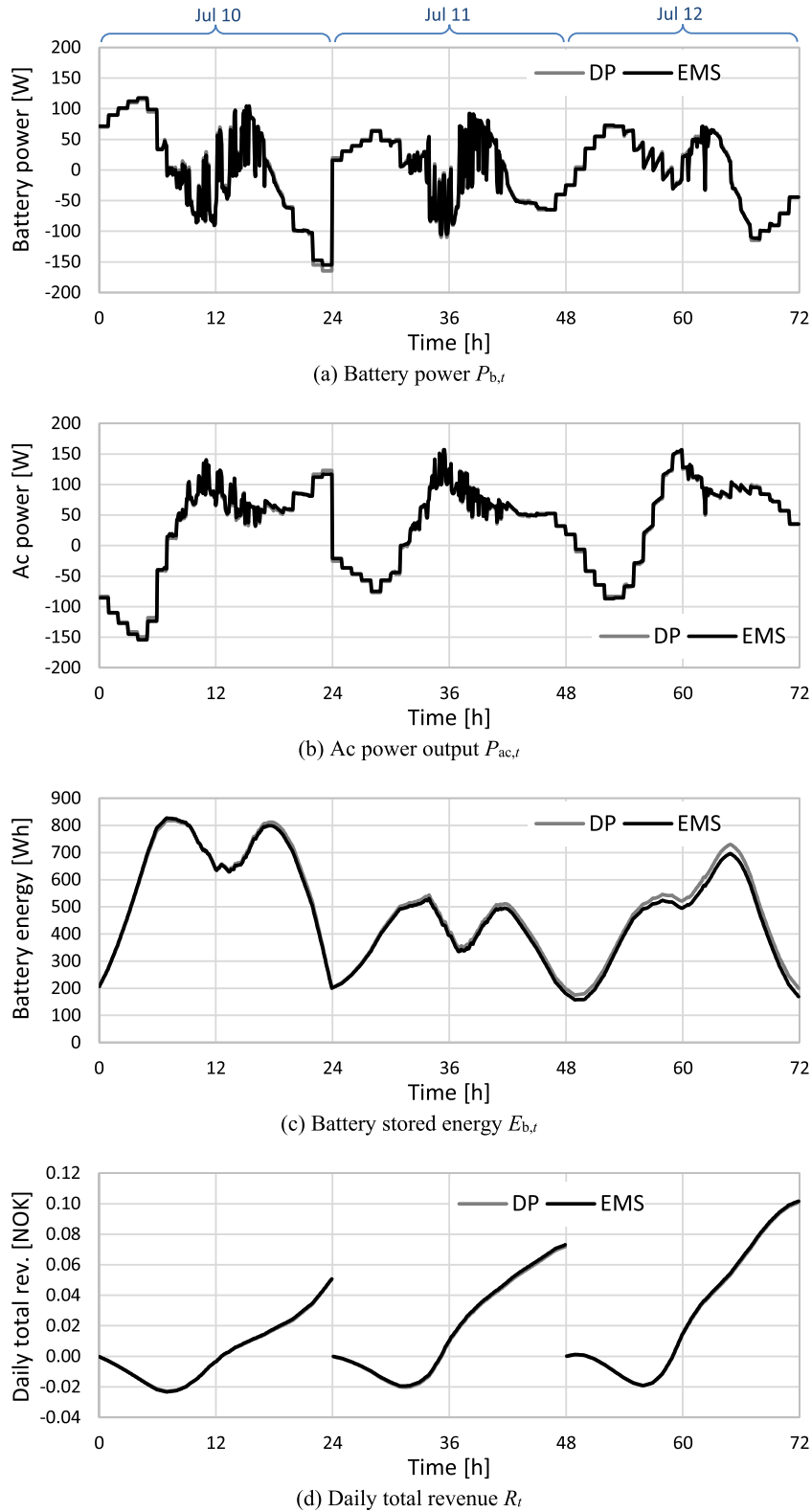
(a) Battery power $P_{b,t}$

(b) Ac power output $P_{ac,t}$

(c) Battery stored energy $E_{b,t}$

(d) Daily total revenue R_t

Fig. 9. Power scheduling simulation results comparing the proposed EMS to the DP method assuming unconstrained battery capacity.

proposes a closed form optimal dispatch function of the battery power as given in (19) and a direct method for estimating the Lagrange multiplier γ as given in (20). The proposed EMS method is verified by benchmarking against the brute-force dynamic programming (DP) approach. The comparative simulation analysis (between the proposed EMS and the brute-force DP approach) first shows that the approximations used in the dispatch function and the Lagrange multiplier estimation yield negligible errors (Fig. 9).
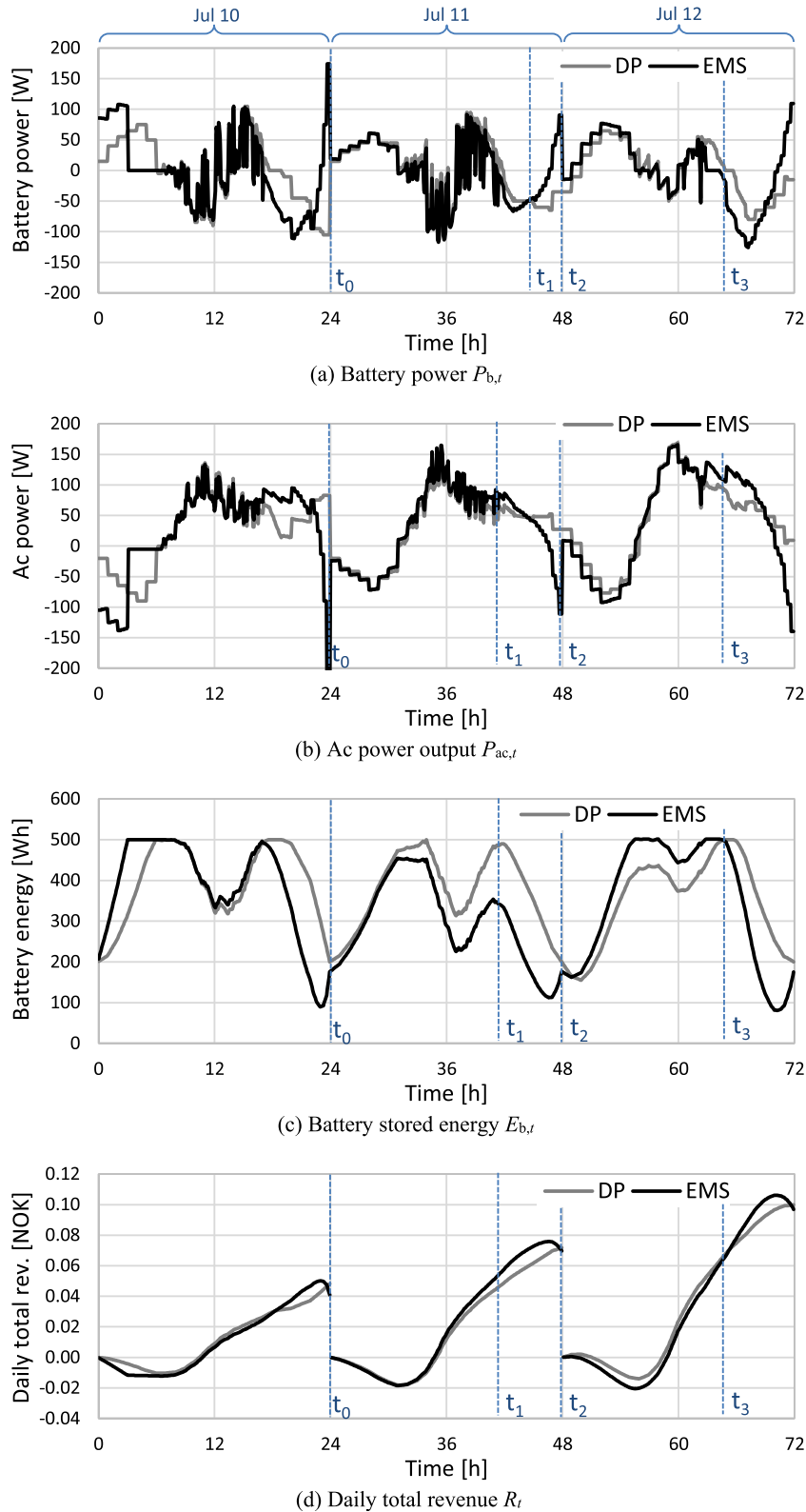
(a) Battery power $P_{b,t}$

(b) Ac power output $P_{ac,t}$

(c) Battery stored energy $E_{b,t}$

(d) Daily total revenue R_t

Fig. 10. Power scheduling simulation results comparing the proposed EMS to the DP method assuming battery capacity is constrained.

Next, the comparative simulation analysis shows that the compensation function as given in (21) can adjust the Lagrange multiplier γ to compensate for the PV power forecasting error. The comparative simulation analysis as given in Fig. 10 shows that the

proposed EMS yields reasonable results in meeting the objective of maximizing the revenue under practical assumptions where the PV power is forecasted and the battery storage capacity is constrained. We may conclude that the proposed EMS presents a practical

approach that is capable of reactively compensating for errors in the forecasting, system modeling or both.

Acknowledgement

Appendix A. Supplementary data

Supplementary data related to this article can be found at https://doi.org/10.1016/j.renene.2018.06.073.

Acronyms and Symbols

BMS	battery management system
DP	dynamic programming
EMS	energy management system
PLL	phase lock loop
PV	photovoltaic
MOSFET	metal−oxide−semiconductor field-effect transistor
MPPT	maximum power point tracker
NOK	Norwegian krone
Wh	watt hour, a unit of energy
C_{pv}	voltage mode photovoltaic controller
C_{ibat}	current mode battery charge controller
C_{vbat}	voltage mode battery charge controller
C_{ff}	feed-forward controller
$E_{b,t,1}$	lower limit of battery stored energy state
$E_{b,t-1,i}$	battery stored energy at state i and time interval $t-1$
$E_{b,t,j}$	battery stored energy at state j and time interval t
$E_{b,t,N}$	upper limit of battery stored energy state
$E_{b,T}$	battery stored energy target over the total optimization time period T
$F_{t,ij}$	maximum total sum of revenue up to time interval t, and at state i
L_{ac}	loss function of ac power path
L_b	loss function of battery power path
$P_{ac,t}$	ac power at time interval t
$P_{b,d}$	average daily battery power
$P_{b,t}$	battery power at time interval t
$P_{br,t}$	battery power target at time interval t
P_d	local demand power
$P_{g,t}$	grid power at time interval t
$P_{p,d}$	average daily photovoltaic power output
$P_{p,t}$	output power of photovoltaic power path at time interval t
P_{pv}	input power to the photovoltaic system
R_t	revenue function at time interval t
R_T	total sum of revenues over the total optimization time period T
t	time interval
T	power scheduling total optimization time period
α, β, χ	coefficients of the loss function of ac power path
Δt	step size of time interval
γ	second Lagrange multiplier
κ	coefficient of the loss function of battery power path
λ	first Lagrange multiplier
$\pi_{g,d}$	daily representative value for the electricity prices
$\pi_{g,t}$	electricity price at time interval t

References

[1] C.L. Masters, Voltage rise: the big issue when connecting embedded generation to long 11 kV overhead lines, Power Eng. J. 16 (Feb. 2002) 5−12.
[2] Y. Ueda, et al., Analysis results of output power loss due to the grid voltage rise in grid-connected photovoltaic power generation systems, IEEE Trans. Ind. Electron. 55 (July 2008) 2744−2751.
[3] J.R. Agüero, S.J. Steffel, Integration challenges of photovoltaic distributed generation on power distribution systems, in: IEEE Power Eng. Soc. General Meeting, San Diego, CA, Jul. 2011.
[4] M. Braun, et al., Optimal reactive power supply in distribution networks − technological and economic assessment for PV-systems, in: Proc. 24th European Photovoltaic and Solar Energy Conf., Hamburg, Germany, Sept. 2009, pp. 3872−3881.
[5] M. Braun, et al., Activation of energy management in households: the novel local consumption tariff for PV-systems and its influence on low voltage distribution grids, in: Proc. Internationaler ETG-kongress/Fachtagung Intelligente Netze, Düsseldorf, Germany, Oct. 2009.
[6] B. Lu, M. Shahidehpour, Short-term scheduling of battery in a grid-connected PV/battery system, IEEE Trans. Power Syst. 20 (2) (May 2005) 1053−1061.
[7] A. Nottrott, et al., Energy dispatch schedule optimization and cost benefit analysis for grid-connected, photovoltaic-battery storage systems, Renew. Energy 55 (July 2013) 230−240.
[8] D. Torres, et al., Scheduling coupled photovoltaic, battery and conventional energy sources to maximize profit using linear programming, Renew. Energy 72 (Dec. 2014) 284−290.
[9] Y. Lu, et al., Optimal scheduling of buildings with energy generation and thermal energy storage under dynamic electricity pricing using mixed-integer nonlinear programming, Appl. Energy 147 (June 2015) 49−58.
[10] Y. Riffonneau, et al., Optimal power flow management for grid connected PV systems with batteries, IEEE Trans. Power Syst. 2 (3) (Nov. 2011) 309−320.
[11] E.L. Ratnam, et al., An optimization-based approach to scheduling residential battery storage with solar PV: Assessing customer benefit, Renew. Energy 75 (March 2015) 123−134.
[12] Y. Iwafune, et al., A comparison of the effects of energy management using heat pump water heaters and batteries in photovoltaic -installed houses, Energy Convers. Manag. 148 (Sept. 2017) 146−160.
[13] M. Urbina, Zuyi Li, A fuzzy optimization approach to PV/battery scheduling with uncertainty in PV generation, in: Proc. 38th North American Power Symp., Sept. 2006, pp. 561−566.
[14] D. Bertsimas, M. Sim, The price of robustness, Oper. Res. 52 (Feb. 2004) 35−54.
[15] A. Charnes, W.W. Cooper, Chance constrained programming, Manag. Sci. 6 (1959) 73−79.
[16] C. Wang, et al., Robust scheduling of building energy system under uncertainty, Appl. Energy 167 (April 2016), 366376.
[17] Q. Wang, et al., A chance-constrained two-stage stochastic program for unit commitment with uncertain wind power output, IEEE Trans. Power Syst. 27 (Feb. 2012) 206−216.
[18] D. Caves, et al., Mitigating price spikes in wholesale markets through market-based pricing in retail markets, The Electicity J. 13 (Apr. 2000) 13−23.
[19] M.H. Albadi, E.F. El-Saadany, Demand response in electricity markets: an overview, in: IEEE Power Eng. Soc. General Meeting, Tampa, FL, Jun. 2007.
[20] L.A. Greening, Demand response resources: who is responsible for implementation in a deregulated market? Energy 35 (Apr. 2010) 1518−1525.
[21] A. Papavasiliou, et al., Market-based control mechanisms for electric power demand response, in: IEEE Conf. Decision and Control, Atlanta, GA, Dec. 2010.
[22] J.B. Cardell, Chin Yen Tee, Distributed energy resources in electricity markets: the price droop mechanism, in: 48th Allerton Conf., Allerton, IL, Sept./Oct. 2010.
[23] S.J. Chiang, et al., Residential photovoltaic energy storage system, IEEE Trans. Ind. Electron. 45 (June 1998) 385−394.
[24] N. Mohan, et al., Power Electronics: Converters, Applications, and Design, third ed., Wiley, Hoboken, NJ, 2003.
[25] F. Hayashi, Econometrics, Princeton University Press, , Princeton, NJ, 2000.
[26] M. Ehrlich, Lithium-ion Batteries, in: Handbook of Batteries, McGraw-Hill, New York, 2002, pp. 67−70 ch. 35, sec. 5,.
[27] R.E. Bellman, S.E. Dreyfus, Applied Dynamic Programming, Princeton University Press, Princeton, NJ, 1962.
[28] A.J. Wood, et al., Economic Dispatch of Thermal Units and Methods of Solution, in: Power Generation, Operation, and Control, Wiley, New York, 2013 ch. 3.
[29] C.L. Nge, O.-M. Midtgård, L.E. Norum, PV with battery in smart grid paradigm: price-based energy management system, in: Proc. 38th IEEE Photovoltaic Specialists Conference (PVSC), Jun. 2012, pp. 575−579.
[30] R. Perez, et al., Validation of short and medium term operational solar radiation forecasts in the US, Sol. Energy 84 (Dec. 2010) 2161−2172.
[31] P. Mathiesen, J. Kleissl, Evaluation of numerical weather prediction for intra-day solar forecasting in the continental United States, Sol. Energy 85 (May 2011) 967−977.
[32] Nord Pool, Market Data: Elspot Day-ahead Prices, 2015 [Online]. Available: http://www.nordpoolspot.com/.